Lawrence Berkeley National Laboratory
Recent Work

Title
ASYMMETRIC SLIP IN Mo SINGLE CRYSTALS

Permalink
https://escholarship.org/uc/item/74z6d09k

Authors
Lau, Silvanus
Dorn, John E.

Publication Date
1969-05-01

ey. 2

ASYMMETRIC SLIP IN Mo SINGLE CRYSTALS

Silvanus Lau and John E. Dorn

May 1969

LAWRENCE RADIATION LABORATORY
UNIVERSITY of CALIFORNIA BERKELEY

DISCLAIMER

ASYMMETRIC SLIP IN Mo SINGLE CRYSTALS

Silvanus Lau[1] and John E. Dorn[2]

Inorganic Materials Research Division, Lawrence Radiation Laboratory,
and Department of Materials Science and Engineering,
College of Engineering, University of California,
Berkeley, California

ABSTRACT

May, 1969

The tensile properties of Mo single crystals in six different orientations were investigated over the range from 20°K to 550°K. The plastic behavior shows asymmetry in the critical resolved shear stress for slip on both {110} planes and {112} planes. At low temperatures, within the thermally activated region, slip seems to take place on well-defined crystallographic planes. At high temperatures in this range, however, slip takes place on irrational planes. The asymmetries associated with yielding and slip increase with decreasing temperature. These effects were rationalized in terms of the modified Peierls model. The model assumes the asymmetric slip arises from a tendency toward asymmetric arrangement of atoms in the core of the $\frac{a}{2} \langle 111 \rangle$ screw dislocation. It is shown that the model can predict with reasonable accuracy the asymmetric stress-temperature-strain rate-orientation relationship and the asymmetric slip behavior.

---

[1]Research Metallurgist and [2]Senior Research Metallurgist, Inorganic Materials Division, Lawrence Radiation Laboratory, University of California, Berkeley, California.

I. INTRODUCTION

Recent experimental investigations on single crystals of bcc metals and alloys have shown that their low-temperature thermally-activated slip behavior is affected by several unique orientation effects. These effects are conveniently described in terms of the angles λ_1, χ_1' and $\lambda_2 \chi_2'$ shown in the standard stereographic projection of Fig. 1. Whereas, λ_1 and λ_2 are the usual Schmid angles between the specimen axis and the [111] or the [$\bar{1}$11] slip directions, χ_1' and χ_2' give the angular deviations of the planes of maximum resolved shear stresses from the ($\bar{1}$01) and the (101) crystallographic planes, respectively. The angles ψ_1 and ψ_2 refer to the angular deviations of the observed slip planes from the ($\bar{1}$01) and the (101) crystallographic planes for slip in the [111] and [$\bar{1}$11] directions respectively. The principal orientation effects are manifested by: (1) Asymmetric critical resolved shear stress laws for yielding. (2) Asymmetric slip band formation. (3) A reversal of the asymmetric behavior upon reversal of the applied stress from tension to compression.

1. <u>Yield Strength.</u> As demonstrated by Taoka, Takeuchai, and Furabayashi[1] on Fe-2.7% Si; Keh and Nakada[2] on Fe; Stein[3] on Mo; Taylor and Christian[4]; Bowen, Christian and Taylor[5] on Nb; Sherwood, Guiu, Kim and Pratt[6] on Ta, Nb, Mo; Argon and Maloof[7] on W; yielding of bcc metals and alloys does not obey the critical resolved shear stress law as originally postulated by Schmid. For example the critical resolved shear stress for slip on the $(\bar{1}01)$ plane in the [111] direction increases as χ'_1 increases when the specimen is tested in tension. Qualitatively the same general trends apply when other slip planes become operative. A schematic representation of this unusual yield behavior is shown in Fig. 2a.

2. <u>Slip Band Formation.</u> The asymmetry of slip band formation has been reported by Taoka et al[1] on Fe-2.7% Si; Sestak, Zarubova and Sladek[8] on Fe-3% Si; Sestak and Zarubova[9] on Fe-6.5% Si and Bowen et al[5] on Nb. The present status of this subject has been reviewed by Kroupa and Vitek[10] and Bowen et al[5]. Slip occurs exclusively in the <111> directions. All recent investigations have failed to confirm the earlier announcements of {123} slip. Slip has been observed to take place on the {101} and {112} planes. A typical case is that for Fe-6.5% Si crystals[9] tested in tension shown in Fig. 2c. For orientations near $\chi'_1 = 0$, slip takes place by the $(\bar{1}01)$ [111] mode and therefore, $\psi_1 = 0$ (vide Fig. 1). At $\chi'_1 = 30$ slip occurs by the $(\bar{2}11)$ [111] mode and therefore, $\psi_1 = 30°$. Over the range of about $25°$ $< \chi'_1 < 30°$, ψ_1 increases from 0 to $30°$ revealing that very intimate $(\bar{1}01)$ to $(\bar{2}11)$ cross slip takes place. At $\chi'_1 = -30°$, slip occurs by the $(\bar{1}\bar{1}2)$ [111] mode and $\psi_1 = -30°$. And between about $-30° \leq \chi'_1 \leq -10°$,

intimate $(\bar{1}\bar{1}2)$ to $(\bar{1}01)$ cross slip occurs. The asymmetric $\psi_1 - \chi_1'$ relationship is clearly revealed in the figure suggesting that when χ_1' is negative cross slip to the $(\bar{1}\bar{1}2)$ plane is more facile than cross slip to the $(\bar{2}11)$ plane when χ_1' is equally positive. In other metals and alloys minor variations are noted from the observations for slip band formation in Fe-6.5% Si. For example, slip takes place in the $[\bar{1}11]$ direction as χ_1' approaches $-30°$ in Nb where the asymmetry is less pronounced than in Fe-6.5% Si.

3. <u>Reversal of Stressing.</u> When the applied stress is changed from tension to compression the asymmetric behavior becomes inverted as shown schematically in Fig. 2.

Several factors are known to affect the degree of asymmetric behavior. Whereas the asymmetric behavior in Nb is quite mild, it is more pronounced in Fe and seems to increase with Si additions to Fe. Mo and W exhibit high degrees of asymmetric behavior. Furthermore, the asymmetric behavior is vanishingly small in the high temperature region where the deformation is athermal and the degree of asymmetric behavior increases as the temperature is lowered in the thermally activated region. Consequently, the asymmetric behavior must be associated with the low-temperature thermally-activated mechanism of deformation in bcc metals.

Escaig[11], Vitek[12], Vitek and Kroupa[13], Kroupa and Vitek[10], Escaig, Fontain, and Friedel[14], Duesberry and Hirsch[15], and Duesberry[16] have suggested several somewhat similar dislocation models in attempts to account for the asymmetric slip behavior in bcc metals. Despite some important differences, all such models were based on one or

another of several assumed asymmetric dissociations of a/2 $\langle 111 \rangle$ screw

dislocations into partial dislocation on several slip planes of their

zone axis. Such sessile dislocations were presumed to slip following

thermally-activated cross slip. The activation energy was calculated

based on the conventional concepts of stacking-fault energies, inter-

action energies between partial dislocation lines and line constriction

energies. The significance of the role of screw dislocations in the

deformation of bcc metals at low temperatures is amply confirmed by their

preponderance over edge dislocations as shown by etch pit investigations

by Low and Guard[17] on Fe-Si; and by electron microscopy by Low and

Turkalo[18] on Si-Fe; Taylor and Christian[4] on Nb; Bowen et al[5] on

Nb; Keh and Nakada[2] on Fe and Swerd[19] on V. Furthermore, some of

the assumed asymmetric dissociations of screw dislocations can account,

at least qualitatively, for the asymmetric slip behavior for thermally

activated deformation at low temperatures. On the other hand, the

predicted effective stress increases much more rapidly with a decrease

in temperature than that observed experimentally. In order to achieve

nominal agreement with the effective stress over the higher range of

temperatures in the low temperature thermally activated range, it is

necessary to assume that stacking fault energies are so high that the

partial dislocations are separated by only about one or two Burgers

vectors. Since at such small separations, the cores of the partial

dislocations must overlap, the analytical treatment of the problem in

terms of stacking-fault energies, interaction energies partial dislocation

lives, and constriction energies is revealed to be inappropriate.

Furthermore, Vitek[20] has recently demonstrated that the various

dissociations of screw dislocation in bcc metals are theoretically untenable. In retrospect, it appears that these probes into the problem of the asymmetric slip behavior of bcc metals are not justified quantitatively and, therefore, serve only to indicate prominent qualitative trends.

Recently Dorn and Mukherjee[21] have suggested an alternate approach for rationalizing the asymmetric slip behavior in bcc metals. They suggested that the stacking fault energies are so high in bcc metals that no true dissociations of the screw dislocations take place. Rather, the tendency toward splitting leads to a decrease in the core energy of the dislocation with a corresponding asymmetric disposition of the core atoms. These concepts are in qualitative agreement with results by Chang[22] and by Bullough and Perrin[23] based on pseudo-potential analyses for the equilibrium positions of atoms about screw dislocations in Fe. In order to move a screw dislocation from one to the next parallel row of atoms on a slip plane, its energy must be increased in a manner somewhat similar to that which applies in the usual Peierls mechanism. The asymmetric arrangement of the core atoms, however, was assumed to be modified by the magnitude and direction of the applied shear stress in such a manner so as to cause the "apparent" Peierls stress to increase as the core atoms are moved in the antitwinning direction. With this innovation, it was possible to reformulate the Dorn-Rajnak[24] model for thermally-activated nucleation of double kinks so as to provide for the asymmetric slip behavior of bcc metals at low temperatures.

Guyot and Dorn[25] have shown that the double-kink model for the

normal Peierls mechanism correlates quite well with the experimental data on low-temperature deformation of polycrystalline bcc metals and on single crystal so oriented that $\lambda_1 \simeq 45°$ and $\chi_1' \simeq 0°$. These correlations are in complete harmony with expectations based on the modified Peierls mechanism. Furthermore, the modified Peierls mechanism[21] was shown to be in nominal agreement with the limited experimental data then available on the effects of crystal orientation on the asymmetric slip phenomenon. The available data, however, were spotty and precluded the possibility of correlating the asymmetry of the yield stress, the asymmetry of slip-band formation and the yield stress-temperature relationship for one metal over the significant temperature range. Furthermore, the range of orientations that had been studied was too limited to permit a detailed comparison of the theory with experiment.

The present investigation was initiated to study in detail the asymmetries of the tensile yield stress and slip band formation as a function of temperature for a wide range of orientations in order to obtain a complete picture of the asymmetric behavior for one material. High purity Mo was selected for this investigation because it is known to exhibit pronounced asymmetric slip behavior.

II. EXPERIMENTAL TECHNIQUE

Commercially "pure" Mo rods were given four passes by the electron-beam zone-refining technique to provide single crystals having less than 100 ppm interstitial impurities. Each rod was seeded to provide a series of about 20 specimens of each orientation shown in the stereographic projection of Fig. 3. The single crystal rods were machined into single crystal specimens each having an 0.80 inch gage length and a 0.125 in. square cross section. The latter was introduced to facilitate two-trace slip-band analyses. After one hour of electro polishing in a H_2SO_4 - CH_3OH solution all surface machining damage, as detected by Laue back-reflection x-ray analysis, was removed. The specimens were then annealed in an ultra-pure He atmosphere at 2000°C to provide a well-annealed initial standard state. The specimens were then given an additional 2-3 minute electropolish which provided a smooth highly-reflective surface that permitted accurate slip-band detection and measurement. Following a final orientation determination the specimens were carefully gauged and then tested in tension at various constant temperatures from 4° to 550°K in an Instron Testing Machine at a strain rate of 3.3 x 10^{-5} per second. The yield stress was determined at an offset of 0.002 strain from the modulus line to an accuracy of better than $\pm$ 3 x 10^6 dynes/cm^2. Specimens were removed at various strains for slip band observations by the Normanski interference contrast technique. Operative slip planes were identified by the two-surface slip-band trace analysis technique.

III. EXPERIMENTAL RESULTS

A. <u>Tensile Yield Stress</u>. Between 450° and 550°K the deformation for all crystal orientations that were investigated was athermal. The yield stresses decreased proportional to the shear modulus of elasticity with increasing temperature. Over this range of temperatures the tensile yield stress, about 1 to 2 x 10^8 dynes/cm^2, was insensitive to crystal orientation. The extremely low values of the athermal yield stresses attest to the high pruity and good crystal perfection that was achieved in this investigation.

The variation of the effective tensile yield stress σ^* (obtained by subtracting the modulus corrected athermal stress level at the test temperature from the experimentally determined tensile yield stress) with temperature, T, for each of the orientations that were investigated is recorded in Fig. 4. The critical temperature Tc, at which the effective yield stress vanished was about 450°K regardless of crystal orientation. As the absolute zero was approached the effective tensile stresses increased to values of 35 to 90 times greater than the athermal stress level dependent on orientation. This reveals that modest variations in the athermal stress level from specimen to specimen, or with crystal orientation, do not significantly affect the effective stress determinations at very low temperatures. Part of the deviations in the σ^* versus T curves with orientation, as will be shown later, arise from differences in the resolved shear stresses on the operative slip planes. The effect of this factor, however, is quite small in contrast to the large differences that were noted in the σ^*-T curves with crystal orientation.

If the Schmid Law (that yielding occurs when the resolved shear stress on the slip plane reaches a critical value) were valid the σ^*-T curves should have increased symmetrically with + or - χ_1' about $\chi_1' = 0$. Consequently the slip behavior is seen to be highly asymmetric. The asymmetry manifests itself by the extraordinarily high tensile yield strengths as χ_1' approaches +30°. Interestingly, the degree of asymmetry is most pronounced at the lowest temperatures and appears to become vanishingly small as T approaches Tc.

B. <u>Slip Band Observations</u>. The operative modes of slip were found to be dependent on crystal orientation, the test temperature and the strain. The general appearance of the slip bands, however, seemed to depend primarily on the test temperature with the expected variation with strain regardless of crystal orientation. Over most of the athermal range from about 450° to 550°K the slip bands were coarse, wavy and branched, indicative of localized slip band formation, and profuse cross slip over macroscopic areas of the slip bands. At about 350°K, however, in the higher-temperature regions of the thermally-activated range, the slip bands were much finer, straight and unbranched. Whereas for some orientations they coincided with low-index rational slip planes for other orientations as will be clarified later, they fell on irrational planes of high indices. At 77°K the slip traces were very fine and closely and uniformly spaced. All traces at 77°K fell on low index rational slip planes. In no case was slip observed to occur on planes of the form {123}. Slip took place only on planes of the forms {110} and {112} or irrational high index planes.

Orientations where χ_1' was positive slipped only by the $a/2$ [111] Burgers vector. As χ_1' was decreased somewhat into the region of negative values, slip also occured via the $a/2$ [$\bar{1}$11] Burgers vector. For orientations where χ_1' was highly negative, slip took place only by the $a/2$ [$\bar{1}$11] Burgers vector.

The most probable slip planes in the zone of the $a/2$ [111] Burgers vector are (0$\bar{1}$1), ($\bar{1}\bar{1}$2), ($\bar{1}$01), ($\bar{2}$11) and ($\bar{1}$10). These, as indicated in Fig. 1, are correlatable with ψ_1 angles of -60°, -30°, 0, +30°, +60° respectively. Analogously, the most probable slip planes in the zone of the $a/2$ [$\bar{1}$11] Burgers vector are (0$\bar{1}$1), (1$\bar{1}$2), (101), (211), and (110) which are characterized by ψ_2 angles of -60°, -30°, 0, +30°, +60° respectively. The observed angles for slip bands at small strains of less than about 0.01 are documented in Table I. The reported angles are estimated to be accurate to about $\pm$ 2°.

With the singular exception of the results given for crystal C, all of the data recorded in Table I are clearly self-explanatory. Whereas, crystal C was very favorably oriented for [111] ($\bar{2}$11) slip, only the [111] ($\bar{1}$01) slip mode was noted at the two lower test temperatures of 77° and 160°K. Clearly [111] ($\bar{2}$11) slip has a higher activation energy than [111] ($\bar{1}$01) slip for this orientation. At the two higher temperatures of 298° and 350°, ψ_1 changed from its 77°K value of 0° to 6° and 15° respectively. This might have resulted from ($\bar{1}$01) and ($\bar{2}$11) cross slip. On the other hand for temperatures above 450°K, two branched and wavey slip bands were predominant, one falling around ψ_1 = 0° and the other around ψ_1 = 60°. There was no evidence for the expected ($\bar{2}$11) mode of slip at any temperature for small strains. Apparently the values of

ψ_1 = 6° and 15° at 298° and 350°K respectively result from ($\bar{1}$01) and ($\bar{1}$10) cross slip.

The data given in Table I revealed that the [111] slip vector can result in slip on the ($\bar{1}$10), ($\bar{1}$01) and ($\bar{1}\bar{1}$2) planes and that the [$\bar{1}$11] slip vector can result in slip on the (0$\bar{1}$1), (1$\bar{1}$2) and (101) planes.

TABLE I

Orientation of Slip Bands

Crystal A: $\lambda_1 = 55°$ $\chi_1' = 16°$ $\lambda_2 = 43°$ $\chi_2' = -30°$

Slip Modes

T in °K	ψ_1	ψ_2	Vector	Principal		Cross Slip With
77	---	-30°	$[\bar{1}11]$	$(1\bar{1}2)$		---
156	---	-30°	"	"		---
298	---	-32°	"	"	and	$(0\bar{1}1)$
425	---	-34°	"	"	and	$(0\bar{1}1)$

Crystal B: $\lambda_1 = 54°$ $\chi_1' = 0°$ $\lambda_2 = 30°$ $\chi_2' = -21°$

Slip Modes

T in °K	ψ_1	ψ_2	Vector	Principal	Cross Slip With
77	0	---	$[111]$	$(\bar{1}01)$	---
298	0	---	"	"	---
325	0	---	"	"	---
356	0	---	"	"	---

Crystal C: $\lambda_1 = 64°$ $\chi_1' = 28°$ $\lambda_2 = 6°$ $\chi_2' = 15°$

Slip Modes

T in °K	ψ_1	ψ_2	Vector	Principal		Cross Slip With
77	0	---	$[111]$	$(\bar{1}01)$		---
100	0	---	"	"		---
298	6°	---	"	"	and	$(\bar{1}10)$
350	15°	---	"	"	and	$(\bar{1}10)$

Crystal D: $\lambda_1 = 44°$ $\chi_1' = 16°$ $\lambda_2 = 39°$ $\chi_2' = 10°$

Slip Modes

T in °K	ψ_1	ψ_2	Vector	Principal	Cross Slip With
77	0	---	[111]	($\bar{1}$01)	---
159	0	---	"	"	---
301	0	---	"	"	---
351	0	---	"	"	---

Crystal E: $\lambda_1 = 45°$ $\chi_1' = -6°$ $\lambda_2 = 39°$ $\chi_2' = -13°$

Slip Modes

T in °K	ψ_1	ψ_2	Vector	Principal	Cross Slip With
77	---	-30	[$\bar{1}$11]	(1$\bar{1}$2)	---
153	-6°		[111]	($\bar{1}$01)	($\bar{1}\bar{1}$2)
		-24°	[$\bar{1}$11]	(1$\bar{1}$2)	(101)
298	-8°		[111]	($\bar{1}$01)	($\bar{1}\bar{1}$2)
		-20	[$\bar{1}$11]	(1$\bar{1}$2)	(101)
352	-10°		[111]	($\bar{1}$01)	($\bar{1}\bar{1}$2)
		-12°	[$\bar{1}$11]	(1$\bar{1}$2)	(101)

Crystal G: $\lambda_1 = 42°$ $\chi_1' = -4°$ $\lambda_2 = 39°$ $\chi_2' = -5°$

Slip Modes

T in °K	ψ_1	ψ_2	Vector	Principal	Cross Slip With
77	0		[111]	($\bar{1}$01)	---
		0	[$\bar{1}$11]	(101)	---
298	-5°		[111]	($\bar{1}$01)	($\bar{1}\bar{1}$2)
		-5°	[$\bar{1}$11]	(101)	(1$\bar{1}$2)
350	-8°		[111]	($\bar{1}$01)	($\bar{1}\bar{1}$2)
		-8°	[$\bar{1}$11]	(101)	(1$\bar{1}$2)

IV. ANALYSIS AND DISCUSSION

It is the objective in this section to attempt to correlate the observed asymmetric slip behavior of Mo single crystals in the low-temperature thermally-activated range of deformation with the modified Peierls model suggested by Dorn and Mukherjee[21]. What need be done is to account for (1) the σ^* - T relationships as a function of orientation, (2) the decreasing degree of asymmetry with increasing temperature, (3) the effect of crystal orientation on the observed slip bands, and (4) the variation of ψ_1 and ψ_2 with temperature.

A. <u>The Asymmetry of the Peierls Stress.</u> A major factor in the theory concerns the assumption that the asymmetric disposition of the atoms in the core of a screw dislocation result in asymmetric Peierls stresses for each permissable mode of slip, with the added feature that the Peierls stress increases when the core atoms are displaced in the antitwinning direction. For example, for the slip planes that were observed to be operative in the present case, the Peierls stresses are given by

$$\tau_{p\bar{1}10} = P_{\bar{1}01} + A_{\bar{1}01} \; \sigma^* \; \cos \lambda_1 \sin \lambda_1 \sin 3\chi_1' \qquad (1a)$$

$$\tau_{p\bar{1}01} = P_{\bar{1}01} + A_{\bar{1}01} \; \sigma^* \; \cos \lambda_1 \sin \lambda_1 \sin 3\chi_1' \qquad (1b)$$

$$\tau_{p\bar{1}\bar{1}2} = P_{\bar{1}\bar{1}2} + A_{\bar{1}\bar{1}2} \; \sigma^* \; \cos \lambda_1 \sin \lambda_1 \sin 3\chi_1' \qquad (1c)$$

for slip by the [111] vector, and by

$$\tau_{p0\bar{1}1} = P_{\bar{1}01} + A_{\bar{1}01} \; \sigma^* \; \cos \lambda_2 \sin \lambda_2 \sin 3\chi_2' \qquad (2a)$$

$$\tau_{p1\bar{1}2} = P_{\bar{1}\bar{1}2} + A_{\bar{1}\bar{1}2} \; \sigma^* \; \cos \lambda_2 \sin \lambda_2 \sin 3\chi_2' \qquad (2b)$$

$$\tau_{p101} = P_{\bar{1}01} + A_{\bar{1}01} \; \sigma^* \; \cos \lambda_2 \sin \lambda_2 \sin 3\chi_2' \qquad (2c)$$

for slip by the [Ī11] vector. The constants $P_{\overline{1}01}$ and $P_{\overline{1}\overline{1}2}$, represent

the Peierls stresses for slip on the indicated planes when χ'_1 (or χ'_2) $=0$.

The constants $A_{\overline{1}01}$ and $A_{\overline{1}\overline{1}2}$ give the degree of asymmetry in the Peierls

stress. This asymmetry, however, depends on how effectively the applied

shear stress $\sigma^* \cos \lambda_1 \sin \lambda_1$ for slip by the [111] vector and

$\sigma^* \cos \lambda_2 \sin \lambda_2$ for slip by the [Ī11] vector displace the core atoms

in the antitwinning direction. This was given by $\sigma^* \cos \lambda_1 \sin \lambda_1 \sin 3\chi'_1$

and $\sigma^* \cos \lambda_2 \sin \lambda_2 \sin 3'_2$ respectively as shown by Eqs. 1 and 2 as a

linear approximation. The value of $P_{\overline{2}11}$ is so high in Mo under tension

that the [111] ($\overline{2}$11) mode is always superceded by other easier modes of

slip.

Although several modes of slip might contribute to the deformation

of single crystals at the higher temperature levels in the thermally

activated range, only one mode of slip can be operative for each

orientation at the absolute zero. It is the mode for which the activation

energy becomes zero first. This generalization accounts for the obser-

vations made in Table I, that the number of slip modes decreases to one

as the temperature is decreased.

The Peierls stress is the resolved shear stress on the operative

slip plane at the absolute zero. This resolution for the cases of

interest here is given by:

$$\tau^*_{1\,\overline{1}10} = \sigma^* \cos \lambda_1 \sin \lambda_1 \cos (60 - \chi'_1) \qquad (3a)$$

$$\tau^*_{1\,\overline{1}01} = \sigma^* \cos \lambda_1 \sin \lambda_1 \cos \chi'_1 \qquad (3b)$$

$$\tau^*_{1\,\overline{1}\overline{1}2} = \sigma^* \cos \lambda_1 \sin \lambda_1 \cos (30 + \chi'_1) \qquad (3c)$$

for slip by the [111] vector, and by:

$$\tau^*_{1\ 0\bar{1}1} = \sigma^* \cos \lambda_2 \sin \lambda_2 \cos (60 + \chi'_2) \tag{4a}$$

$$\tau^*_{1\ 1\bar{1}2} = \sigma^* \cos \lambda_2 \sin \lambda_2 \cos (30 + \chi'_2) \tag{4b}$$

$$\tau^*_{1\ 101} = \sigma^* \cos \lambda_2 \sin \lambda_2 \cos \chi'_2 \tag{4c}$$

for slip by the $[\bar{1}11]$ vector. Whereas the last three subscripts on τ refer to the slip plane, the first subscript 1 or $\bar{1}$ refers to the slip vector [111] or $[\bar{1}11]$. Extrapolating the experimental value of the stress σ^* as given in Fig. 4 to the absolute zero and resolving it on the operative low-temperature slip plane and plotting it as a function of $\sigma^* \cos \lambda_1 \sin \lambda_1 \cos 3\chi'_1$ or $\sigma^* \cos \lambda_2 \sin \lambda_2 \cos 3\chi'_2$, dependent on which is appropriate, gives the solid circles in Fig. 5. Clearly the linear approximation suggested by Eqs. 1a, 1b, and 2a for the Peierls stress for $\{101\}$ slip is excellent and gives values of $A_{\bar{1}01}$ of 0.263 and $P_{\bar{1}01}$ of about 45 x 10^{-8} dynes/cm^2. The two solid datum squares for $\{112\}$ slip exhibit a lesser slope. In order to obtain a better estimate of the slope the open datum points were calculated for the resolved shear stresses on non-operative planes. Obviously the corresponding Peierls stress for these planes is above the open datum points. Thus, $\{112\}$ slip is seen also to exhibit asymmetry but the value of $A_{\bar{1}\bar{1}2}$ is estimated to be only about 0.125 or slightly less and $P_{\bar{1}\bar{1}2}$ is about 40.2 x 10^{-8} dynes/cm^2. The significant correlations revealed in Fig. 5 could not be made previously because the existing data was then far too limited in scope.

B. <u>Slip Bands and Their Asymmetries.</u> Slip bands arise only from those modes of deformation that have relatively high frequencies of activation. At very low temperatures, as was previously discussed,

slip will take place only by that mode for which the activation energy first vanished with increasing stress. A major factor that determines the operative mode is crystal orientation. The increasing amounts of cross slip and the introduction of slip by new slip vectors as the temperature is increased must be ascribed to the increased frequency of activation of such modes of deformation. In this section of the report an attempt will be made to rationalize the observed asymmetric slip band formations and their variations with temperature. The analysis will be based on an extension of the Dorn-Rajnak[24] model for the activation of slip by the nucleation of double kinks.

The activation energy for the nucleation of a pair of kinks, Un, is given by [21,24,25]

$$Un = 2 \, U_k \, f\left\{\frac{\tau^*}{\tau}\right\} \tag{5}$$

where U_k is the full kink energy under zero effective stress, τ^* is the effective shear stress on the operative slip plane and τ_p is the corresponding Peierls stress. The function $f\{\tau^*/\tau_p\}$ varies from zero when $\tau^*/\tau_p = 1$ to unity when $\tau^*/\tau_p = 0$ and depends only mildly on the shape of the Peierls hill. In their formulation of the modified Peierls mechanism Dorn and Mukherjee[21] employed the f function appropriate to a sinusoidal Peierls hill. It appears, however, that the quasi-parabolic Peierls hill described by Guyot and Dorn[25] might be more appropriate for the asymmetric core model of the modified Peierls mechanism. The predicted τ^*/τ_p versus T/Tc curve for crystal B, which exhibited exclusively [111] ($\bar{1}$01) slip over the entire thermally activated range of temperatures, agreed very well with the experimental data when the

energy to nucleate a double kink was selected to be

$$U_n = \alpha \, \pi \, a \, \sqrt{\frac{ab\tau_p \Gamma}{8}} \left\{ 1 - \frac{\tau^*}{\tau_p} \right\}^{1.85} \tag{6}$$

where α is 1.92, a is the spacing between parallel rows of atoms on the slip plane, b is the Burgers vector and Γ is the energy of a unit long screw dislocation. This differs only slightly from the theoretical expression of Un for the quasi-parabolic Peierls hill for which the modifying factor $\alpha \simeq 1$ in lieu of 1.92, and the exponent of the bracketed term is 2 in lieu of 1.85.

It is expected that the Peierls hills for the various modes of slip differ from each other. The major factors responsible for such deviations are known[25] to be the magnitude of the Peierls stress, τ_p the value of the kink height, a, and α. In general, however, the trends are rather insensitive to small variations in the exponent of the bracketed term of Eq. 5 and for that reason the value of 1.85 will be used for all modes of slip observed here.

Since the values of α, a, and τ_ρ depend on the mode of slip, the activation energy for slip by the [111] vector on the (h k 1) plane will be represented by

$$U_{1hkl} = \alpha_{hkl} \, \pi a_{hkl} \sqrt{\frac{a_{hkl} b \tau_{p1hkl} \Gamma}{8}} \left\{ 1 - \frac{\tau^*_{1hkl}}{\tau_{p1hkl}} \right\}^{1.85} \tag{7}$$

The symbol 1 is replaced by $\bar{1}$ when slip occurs by the [$\bar{1}$11] vector.

It has been shown[24] that the frequency for activation on any (hkl) plane of bcc crystal by the [$\overset{\shortmid}{1}$11] vector is given by

$$\nu^*_{1hkl} = \frac{\nu^2_{1hkl}}{\nu_{1\bar{1}10} + \nu_{1\bar{2}11} + \nu_{1\bar{1}01} + \nu_{1\bar{1}\bar{1}2} + \nu_{1110}} \tag{8}$$

with a similar expression for slip by the $[\bar{1}11]$ vector. The frequency $\nu_{_1hkl}$, previously derived for the quasi-parabolic hill, is given by

$$\nu_{_1hkl} = \frac{\nu_o \, b^2 \, L_{_1} \, \tau_{p_1hkl}}{\pi^2 \, a_{hkl} \, \Gamma} \, e^{-\left(\frac{U_{_1hkl}}{kT}\right)} \qquad (9)$$

where ν_o is the Debye frequency and L_1 is the length of the $[111]$ dislocation segment that is advanced to the most parallel row of atoms. For the observed slip planes in Mo single crystals in this investigation, the frequency expressions reduce to

$$\nu^*_{_1hkl} = \frac{\nu^2_{_1hkl}}{\nu_{_{1110}} + \nu_{_{1101}} + \nu_{_{1112}}} \qquad (10)$$

and

$$\nu^*_{_1hkl} = \frac{\nu^2_{_1hkl}}{\nu_{_{\bar{1}1\bar{1}0}} + \nu_{_{\bar{1}10\bar{1}}} + \nu_{_{\bar{1}112}}} \qquad (11)$$

for the $[111]$ and the $[\bar{1}11]$ slip vectors respectively.

Simple vector analysis[24] gives the angles ψ_1 and ψ_2 that the slip bands produced by the $[111]$ and $[\bar{1}11]$ slip vectors respectively. For the operative slip modes in Mo single crystals these reduce to

$$\cot \psi_1 = \frac{\frac{1}{2} \nu^*_{_{1\bar{1}10}} \, a_{_{1\bar{1}0}} + \nu^*_{_{1\bar{1}01}} \, a_{_{1\bar{1}01}} + \sqrt{3}/2 \, \nu^*_{_{1\bar{1}12}} \, a_{_{112}}}{\sqrt{3}/2 \, \nu^*_{_{10\bar{1}1}} \, a_{_{01\bar{1}}} - \frac{1}{2} \nu^*_{_{1\bar{1}12}} \, a_{_{11\bar{2}}}} \qquad (12a)$$

$$\cot \psi_2 = \frac{\frac{1}{2} \nu^*_{_{\bar{1}0\bar{1}1}} \, a_{_{0\bar{1}1}} + \sqrt{3}/2 \, \nu^*_{_{\bar{1}1\bar{1}2}} \, a_{_{1\bar{1}2}} + \nu^*_{_{\bar{1}101}} \, a_{_{10\bar{1}}}}{\sqrt{3}/2 \, \nu^*_{_{\bar{1}0\bar{1}1}} \, a_{_{0\bar{1}1}} - \frac{1}{2} \nu^*_{_{\bar{1}1\bar{1}2}} \, a_{_{1\bar{1}\bar{2}}}} \qquad (12b)$$

The predicted values of ψ_1 and ψ_2 were obtained as follows:

1. The Peierls stresses are given by Eqs. 1 and 2 into which were introduced the experimentally determined values of $P_{\bar{1}01} = 45.0 \times 10^8$ dynes/cm^2, $A_{\bar{1}01} = .263$, $P_{\bar{1}\bar{1}2} = 40.2 \times 10^{+8}$ dynes/cm^2 and $A_{\bar{1}\bar{1}2} = .125$, as recorded in Fig. 5.

2. The effective shear stresses τ^* were calculated in terms of the applied tensile stress, σ^*, and crystal orientation as required by Eqs. 3 and 4.

3. The following values were employed for the designated parameters:

$b = 2.73 \times 10^{-8} cm$

$A_{\bar{1}01} = 2 \quad 2 b/3$

$A_{\bar{1}\bar{1}2} = 6 \quad b/3$

$G = 1.296 \times 10^{12} dynes/cm^2$

4. The value of $\alpha_{\bar{1}01}$, which must be the same for all $\{101\}$ planes, was obtained from the effect of strain rates on Tc as reported previously[26] for crystal B which slipped exclusively by the [111] $(\bar{1}01)$ mode. Since $2U_{k\bar{1}\bar{1}01}$ was found to be $1.98 \times 10^{-12} ergs$, $\alpha_{\bar{1}01} = 1.92$.

5. Since more of the tested orientations gave exclusively the [111] $(\bar{1}\bar{1}2)$ slip mode, the above mentioned technique could not be used to determine $\alpha_{\bar{1}\bar{1}2}$. It was shown to be $\alpha_{\bar{1}\bar{1}2} = 2.7$ from the value of $\cot \psi_1$ Eq. 12a, for crystal E.

Having in this way established all of the pertinent physical constants, ψ_1 and ψ_2 of Eqs. 12 a and b were calculated by introducing the appropriate values which are given by the physical constants given above into Eqs. 7, 8 and 9. The calculated values shown by the solid lines, are compared in Fig. 6 with the experimental data, shown by datum points. The correlation between the modified Peierls mechanism for asymmetric cores and the slip band data and its variation with temperature is rather good, and need not be elaborated further. It is important to note, however, that the calculated variation of ψ_1 with temperature for crystal C was based on the assumed $(\bar{1}01)$ to $(\bar{1}10)$ cross slip and not on $(\bar{1}01)$ to $(\bar{2}11)$ cross slip.

IV. THE EFFECTIVE YIELD STRESS

A major factor in evaluating the possible validity of any thermally-activated dislocation model centers about the agreement that is obtained between the predicted variation of yield stress with temperature and that obtained experimentally. In the case of bcc metals, such as Mo, which appear to have asymmetric arrangements of atoms in the dislocation core, the resolved shear stress at yielding is inappropriate for this comparison: 1.) For example, the experimental effective yield stress-temperature data given in Fig.4 clearly reveals that the critical resolved shear stress criterion for yielding is not obeyed. 2.) Furthermore, as shown by the previously described slip band analysis, a given dislocation can undertake intimate cross slip from one operative plane to another. 3.) The amount of such cross slip depends not only on crystal orientation, but also on the test temperature. 4.) And finally several different slip vectors might be operative at one time dependent on crystal orientation and temperature. These issues can be avoided by direct formulation of the tensile strain rate as a function of the tensile stress[24] by tension resolution of the shear strain rates of each operative mode of slip to give the total tensile strain rate.

Following the analysis of Dorn and Mukherjee[21], the shear strain rates on the (hkl) planes are given by

$$\dot{\varepsilon}_{1hkl} = \rho_1 \, ba_{hkl} \, v^*_{1hkl} \tag{13a}$$

and

$$\dot{\varepsilon}^-_{1hkl} = \rho^-_1 \, ba_{hkl} \, v^{*-}_{1hkl} \tag{13b}$$

where ρ_1 and ρ^-_1 are the densities of screw dislocations having the [111]

and the $[\bar{1}11]$ slip vectors respectively. For the operative slip
mechanisms in Mo the tensile $\dot{\varepsilon}$ strain rate then becomes

$$\dot{\varepsilon} = \cos \lambda_1 \sin \lambda_1{}' \{ \dot{\varepsilon}_{\bar{1}1\bar{1}0} \cos(60 - \chi_1{}') + \dot{\varepsilon}_{\bar{1}10\bar{1}} \cos \chi_1{}' + \dot{\varepsilon}_{\bar{1}1\bar{1}2} \cos(30 +$$

$$\chi_1{}') \} + \cos \lambda_2 \sin \lambda_2 \{ \dot{\varepsilon}_{10\bar{1}\bar{1}} \cos(60 + \chi_2{}') + \dot{\varepsilon}_{\bar{1}1\bar{1}2} \cos(30 + \chi_2{}')$$

$$+ \dot{\varepsilon}_{\bar{1}10\bar{1}} \cos \chi_2{}' \} \tag{14}$$

In order to facilitate the analysis, it was assumed that $\rho_1 L_1 = \rho_1 L_1 = \rho L$
whenever duplex slip took place. Although the validity of this
assumption might be questioned, the issue is not critical for evaluating
the $\sigma^* - T$ relationship because σ^* and T appear as strong variables in
the exponential term of the equations, whereas ρL appears as a weak
variable in the pre-exponential term. For a given test all quantities
such as $\dot{\varepsilon}$, σ^*, τ_p, etc, pertinent to the application of Eq. 14 are known
excepting $\rho L \nu_0$. These values were calculated for each crystal by
introducing the known data at $77°K$ where only one slip system was
operative. In view of the insensitivity of $\sigma^* - T$ relationship to the
value of $\rho L \nu_0$, the variations of $\rho L \nu_0$ from crystal to crystal were small.
Employing these values the solid predicted curves shown in Figs. 7a and
7b, σ^* versus T were obtained. These can be compared directly with the
corresponding experimental datum points as shown.

In addition to the theoretical formulation of the modified Peierls
mechanism, the predicted curves were based on only the following
experimental data: 1.) The asymmetric Peierls stresses, shown in Fig. 5,
obtained by extropolating the yield stress for each orientation to the
absolute zero. 2.) The slip band that was operative for each orientation
at low temperatures. 3.) The value of $\alpha_{\bar{1}01}$ as deduced from the

experimentally established kink energy which was determined from the effect of strain rate on Tc for crystal B. 4.) The value of $\alpha_{\overline{112}}$ as deduced from slip band observations on Crystal E. 5.) The average value of $\rho L \nu_o$ as deduced from the known values of $\dot{\varepsilon}$ and σ^* at $77^\circ K$ for each crystal. 6.) No arbitrary adjustments were made. 7.) All experimentally determined quantities were in good agreement with theoretical expectations.

The agreement between the predicted and experimentally determined σ^* - T curves, although not perfect is nevertheless quite good. It is seen that the assumption of an asymmetric Peierls stress, vide Fig. 5, which is the principal concept involved, does account qualitatively for the asymmetries that are present in the σ^* - T curves. Furthermore, the decrease in the asymmetric behavior with increasing temperature is automatically accounted in the assumption that τ_p depends on the orientation and magnitude of the applied shear stress in a manner suggestive of changes in the arrangement of atoms in the dislocation core. When the applied stress tends to move atoms in the antitwinning direction the Peierls stress, and consequently the yield stress, increases for all operative slip planes at all temperatures. This effect seems to be so strong in Mo single crystals so as to preclude the operation of [111] ($\overline{2}11$) slip for positive values of χ_1', whereas, in contrast [111] ($\overline{1}\overline{1}2$) slip occurs with relative ease for negative values of χ_1'. The agreement between the predicted and experimentally determined σ^*-T curves is excellent near $\chi_1' = 0$. For values of χ_1' near + 30° and to a lesser degree for those of χ_1' near - 30°, the agreement is not as good. Several factors, such as the assumed linear variation of the Peierls

stress with $\sigma^* \cos \lambda_1 \sin \lambda_1 \sin 3\chi'$, the assumption that the shapes of the Peierls hills are about the same for $(\bar{1}\bar{1}2)$ and $(\bar{1}01)$ slip, and the assumption that the shapes of the Peierls hill does not depend on $\sigma^* \cos \lambda_1 \sin \lambda_1 \sin 3\chi_1'$.

The correlations presented here call for more intensive effort on determining the lowest energy configurations of atoms in the core of screw dislocation in bcc metals, their displacements under applied stresses, and the details of the minimum energy for their thermally-activated motion when a double kink is formed. The completion of such approaches, however, appear at present to constitute a series of formidable tasks which may not be adequately done for many years. In the interim less pretentious approaches such as that provided by the simple modified Peierls model might prove useful.

V. CONCLUSIONS

1. From 450°K to 550°K the deformation of Mo single crystals is athermal. All orientations gave approximately the same low yield stress of about 1 to 2 x 10^8 dynes/cm^2 and exhibit similar coarse, wavy and branched types of slip bands indicative of polyslip, and extensive cross slip. Asymmetric behavior, if present at all, was so minor as to be undetectable.

2. Between 450° and 20°K thermally activated slip deformation took place. The effective yield stress increased rapidly with decreasing test temperatures and the slip bands became finer and sharper. At the lowest temperatures, slip took place on planes of the forms {101} and {112}. At higher temperatures slip occured on irrational planes illustrative of cross slip and for some orientations duplix slip was observed. Slip never occured by the [111] ($\bar{2}$11) mode even for orientations extremely favorable for the operation of this mode. In contrast slip did take place by the [111] ($\bar{1}\bar{1}$2) mode even for some orientations that were not especially favorable for this mode. Thus, slip band formation was strikingly asymmetric.

3. The critical resolve shear stress law was found to be invalid resulting in highly asymmetric yield stress. The degree of asymmetry for both slip band formation and the yield stress decreased as the temperature was increased.

4. The asymmetric behavior was analyzed in terms of a modified Peierls mechanism of slip base on the nucleation of double kinks on screw dislocations in bcc metals. It was found that this model provided a good qualitative description of the origin of the asymmetric thermally-activated slip behavior of Mo.

ACKNOWLEDGEMENTS

REFERENCES

1. T. Taoka, S. Takeuchi and E. Furubayashi; J. Phys. Soc., Japan, 1964, Vol. 19, p. 701.

2. A. S. Keh and Y. Nakada; Canad. J. Phys., 1967, Vol. 45, No. 2, Part 3, p. 1101.

3. D. F. Stein; Canad. J. Phys., 1967, Vol. 45, No. 2, Part 3, p. 1063.

4. G. Taylor and J. W. Christian; Phil. Mag., 1967, Vol. 15, p. 873.

5. D. K. Bowen, J. W. Christian and G. Taylor; Canad. J. Phys. 1967, Vol. 45, No. 2, Part 3, p. 903.

6. P. J. Sherwood, F. Guiu, H. C. Kim and P. L. Pratt; Canad. J. Phys., 1967, Vol. 45, No. 2, Part 3, p. 1075.

7. A. S. Argon and S. R. Maloof; Acta. Met., 1966, Vol. 14, p. 1449.

8. B. Sestak, N. Zarubova and V. Sladek; Canad. J. Phys., 1967, Vol. 45, No. 2, Part 3, p. 1031.

9. B. Sestak and N. Zarubova; Phys. Stat. Sol., 1965, Vol. 10, p. 239.

10. F. Kroupa and V. Vitek; Canad. J. Phys., 1965, Vol. 45, No. 2, Part 3, p. 945.

11. B. Escaig; J. Phys., 1966, Vol. 27, C3-205.

12. V. Vitek; Phys. Stat. Sol., 1967, Vol. 22, p. 453.

13. V. Vitek and F. Kroupa; Phys. Stat. Sol., 1966, Vol. 18, p. 703.

14. B. Escaig, G. Fontain and J. Friedel; Canad. J. Phys., 1967, Vol. 45, No. 2, Part 2, p. 481.

15. M. S. Duesbery and P. B. Hirsch; Dislocation Dynamics (McGraw-Hill, N.Y., 1968) p. 57.

16. M. S. Duesberry; Phil. Mag., 1969, Vol. 19, No. 159, p. 501.

17. J. R. Low and R. W. Guard; Acta. Met., 1959, Vol. 7, p. 171.

18. J. R. Low and A. M. Turkalo; Acta. Met., 1962, Vol. 10, p. 215.

19. P. Smerd; D. Phil. Dissentation, 1968, Univ. of Oxford.

20. V. Vitek; Phil. Mag., 1968, Vol. 18, No. 154, p. 773.

21. J. E. Dorn and A. K. Mukherjee; Trans. AIME. to be published.

22. R. Chang; Phil. Mag., 1967, Vol. 16, p. 1021.

23. R. Bullough and R. C. Perrin; Dislocation Dynamics, (McGraw-Hill, N.Y., 1968) p. 175.

24. J. E. Dorn and S. Rajnak; Trans. Met. Soc. AIME., 1964, Vol. 230, p. 1052.

25. P. Guyot and J. E. Dorn; Canad. J. Phys., 1967, Vol. 45, No. 2, Part 3, p. 983.

26. S. S. Lau, S. Rauji, A. K. Mukherjee, G. Thomas, and J. E. Dorn, Acta. Met., 1967, Vol. 15, p. 237.

FIG. I STANDARD STEREOGRAPHIC PROJECTION.
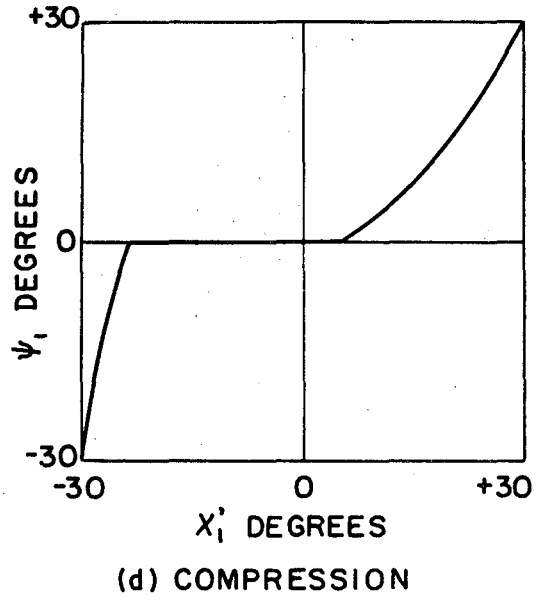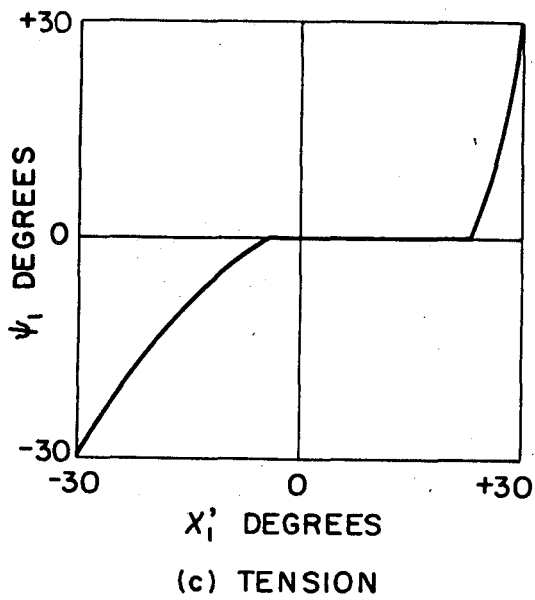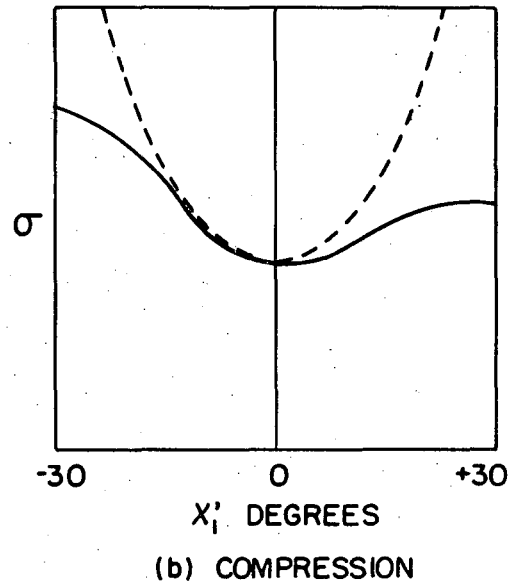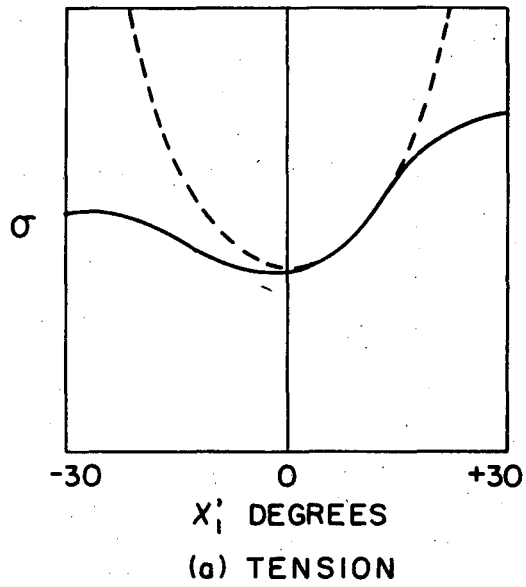
XBL 695-523

FIG. 2 SCHEMATIC REPRESENTATION OF ASYMMETRIC
BEHAVIOR.
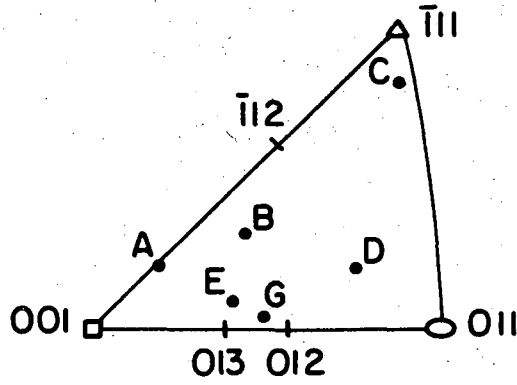
FIG. 3 ORIENTATIONS OF THE SPECIMENS.
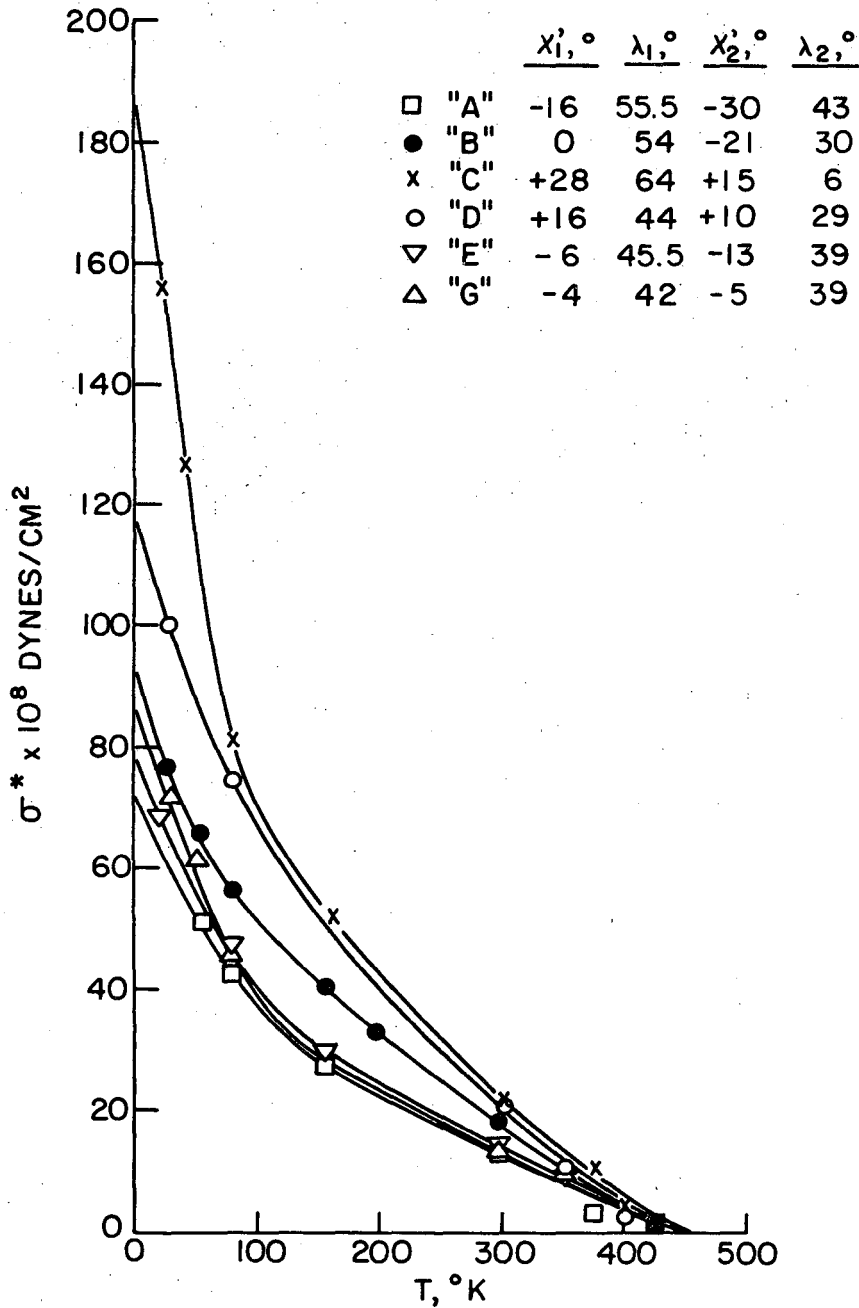
FIG. 4 THE EFFECTIVE TENSILE YIELD
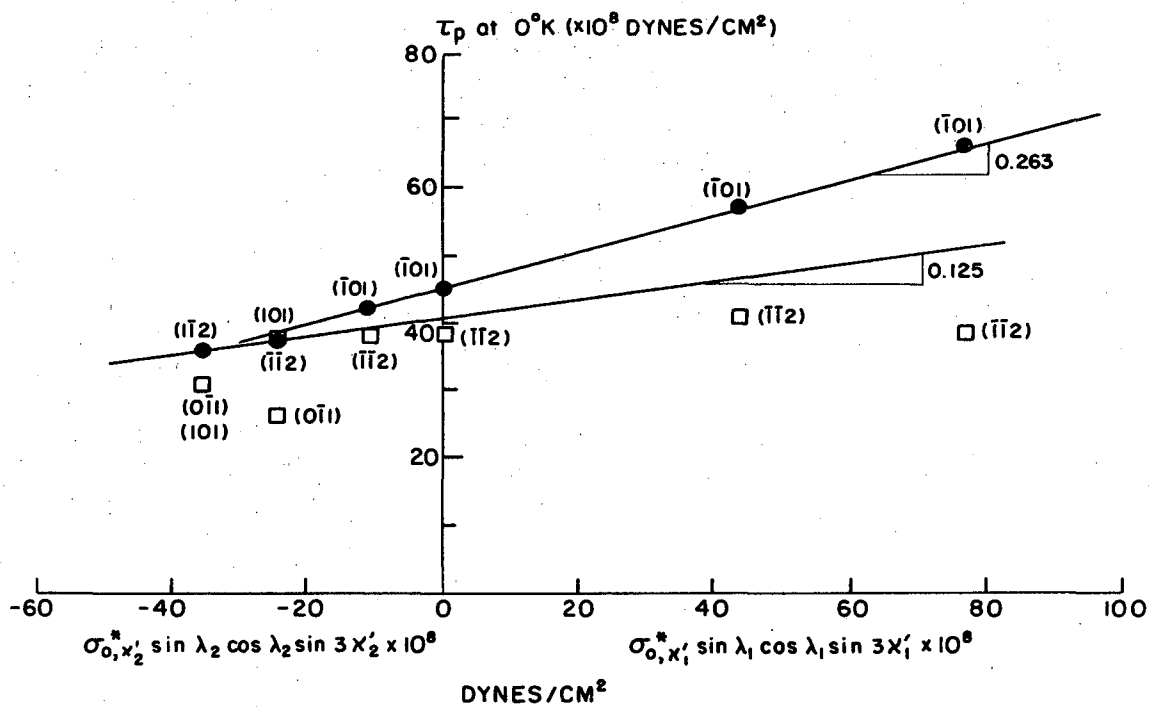STRESS FOR VARIOUS ORIENTATIONS AS
A FUNCTION OF TEMPERATURE.

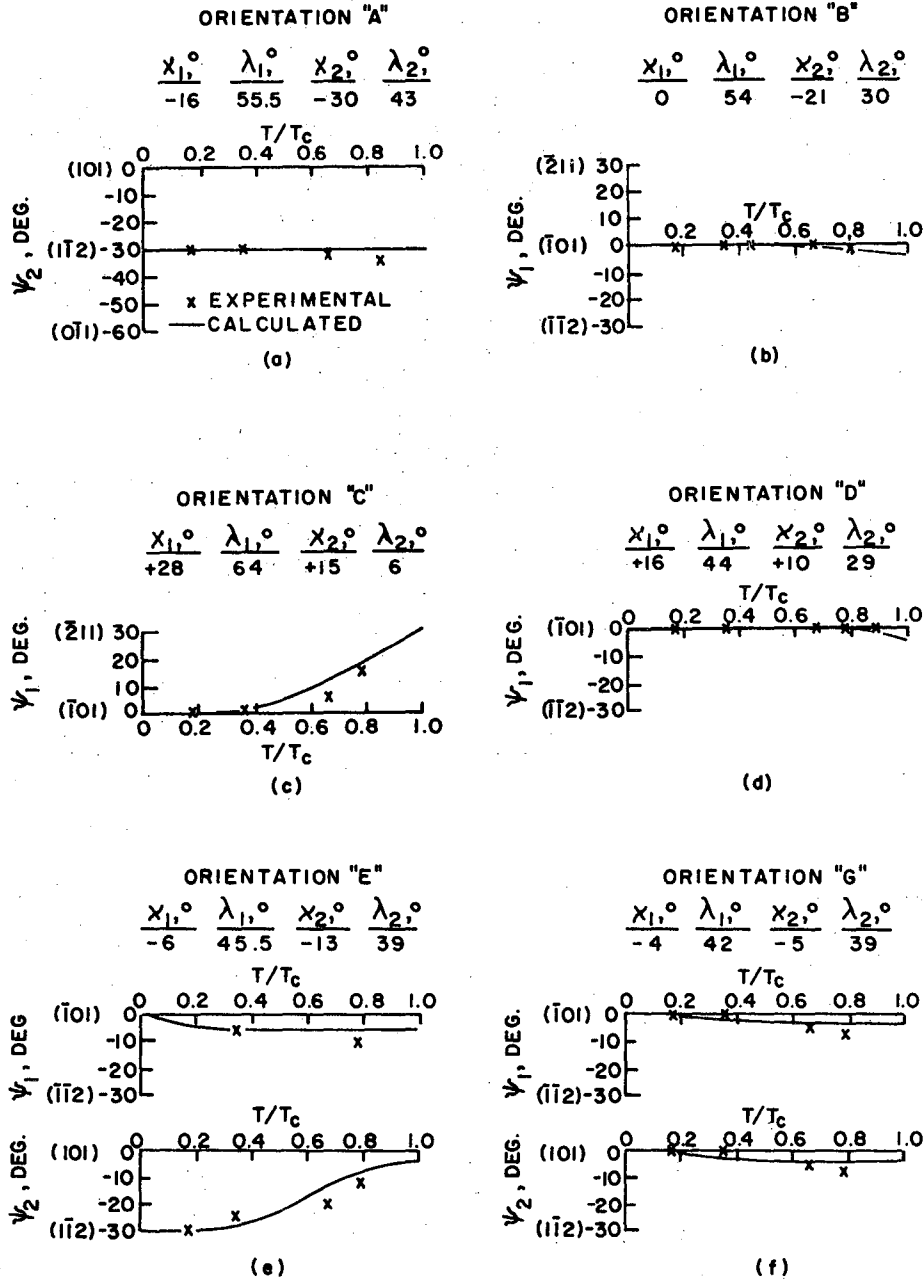XBL 695-526

FIG. 5 PEIERLS STRESSES AT 0°K.

ORIENTATION "A"
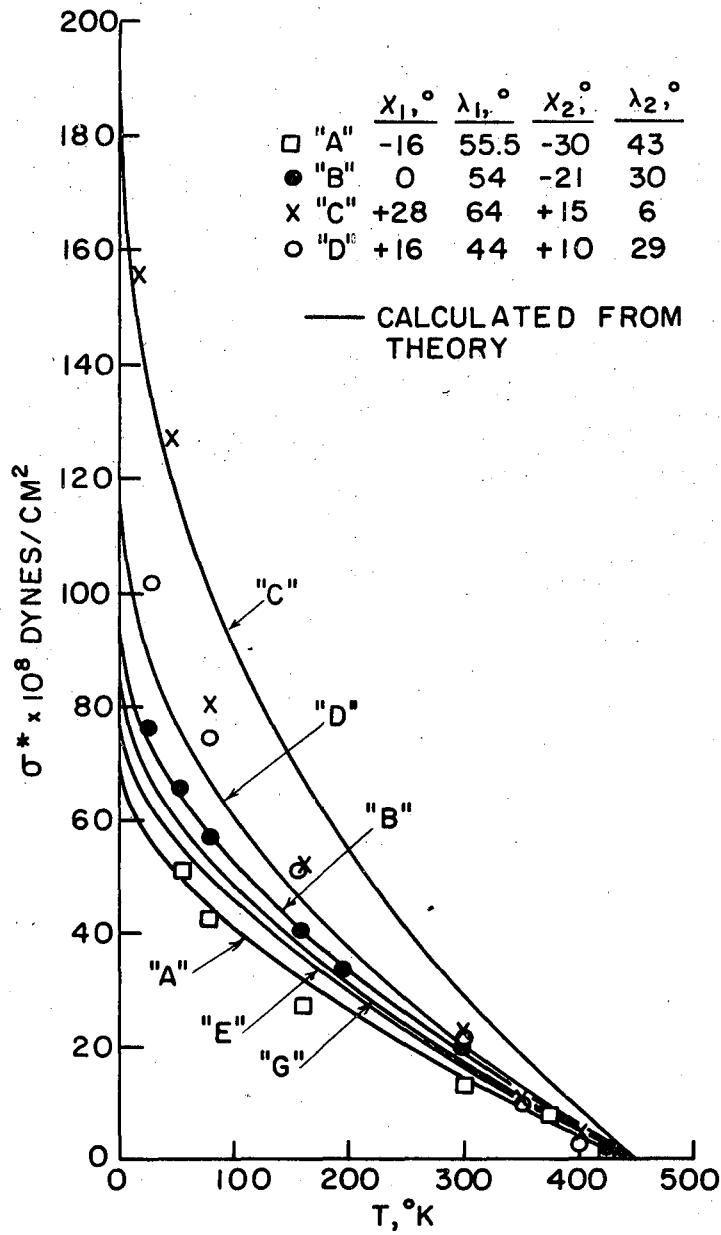
$\chi_1,^\circ$	$\lambda_1,^\circ$	$\chi_2,^\circ$	$\lambda_2,^\circ$
-16	55.5	-30	43

ORIENTATION "B"

$\chi_1,^\circ$	$\lambda_1,^\circ$	$\chi_2,^\circ$	$\lambda_2,^\circ$
0	54	-21	30

(a)

(b)

ORIENTATION "C"

$\chi_1,^\circ$	$\lambda_1,^\circ$	$\chi_2,^\circ$	$\lambda_2,^\circ$
+28	64	+15	6

ORIENTATION "D"

$\chi_1,^\circ$	$\lambda_1,^\circ$	$\chi_2,^\circ$	$\lambda_2,^\circ$
+16	44	+10	29

(c)

(d)

ORIENTATION "E"

$\chi_1,^\circ$	$\lambda_1,^\circ$	$\chi_2,^\circ$	$\lambda_2,^\circ$
-6	45.5	-13	39

ORIENTATION "G"

$\chi_1,^\circ$	$\lambda_1,^\circ$	$\chi_2,^\circ$	$\lambda_2,^\circ$
-4	42	-5	39

(e)

(f)

FIG. 6   THE SLIP BAND GEOMETRY.

XBL 695-528

FIG. 7a COMPARISON OF PREDICTED EFFECTIVE
YIELD STRESS FOR VARIOUS ORIENTATIONS AS
A FUNCTION OF TEMPERATURE WITH THE
EXPERIMENTAL DATUM POINTS.

FIG. 7b COMPARISON OF PREDICTED EFFECTIVE
YIELD STRESS FOR VARIOUS ORIENTATIONS AS
A FUNCTION OF TEMPERATURE WITH THE
EXPERIMENTAL DATUM POINTS.